Anonymous Referee #1

Major comments

1. The authors only mention the datasets used for meteorological initial and boundary conditions in Section 2.2. However, the chemical initial and boundary conditions are also needed for driving the regional chemistry transport model. It is necessary to clarify datasets for this purpose.

Response: The monthly mean values of all tracers from observation data are used for initialization at the very beginning of the model run. The initial values of all gases in RADM2 and aerosol concentrations are based on the 24 h forecast made by the previous day's model run. This has been added in the manuscript.

2. Another regional high PM2.5 event occurred on 24-25 in the same month according to observational data shown in Fig.4. I am wondering why the authors did not analyze this episode even they already ran the model for the entire month. In my opinion the analysis include the both episodes certainly makes the study stronger.

Response: We have already finished the simulations of the whole 2013-2014 winter and chose one haze as the case study of the PM2.5 pollutant transportation in this paper. PM2.5 transport study of the whole 2013-2014 winter will be analyzed in next paper, which need more model evaluation including meteorology and PM2.5.

3. In order to identify the transport contribution to PM2.5 levels in Beijing (PK), the authors estimate the horizontal advective fluxes of PM2.5 with a box covering PK. But it is hard to conclude that "the remaining 1230t could be attributed to local emissions" at Line 11 on Page 3757 because sinks (e.g. dry and wet deposition) and sources (e.g. emission and chemical transformation) are not involved the authors' calculations. Therefore this method cannot quantitatively decouple the contribution of transport process from final results determined by all processes.

Response: Sinks (e.g. dry and wet deposition), emissions and chemical transformations were all calculated in the model dynamic, physical and chemical processes in every model step, 1230t is the difference between the total increasing amount of suspended PM2.5 and transport amount from surroundings of BJ, which may be mainly caused by local reasons.

"The remaining 1230t could be attributed to local emissions" is not exact and should be changed into "The remaining 1230t suspended in the atmosphere over BJ could be attributed to local effects ".

4. Due to the aerodynamic effects of large scale topography on the regional wind field, it is not surprising to me the spatial distribution pattern of PM2.5 is clearly dependent on topography over the Eastern China. The authors may analyze topographic influences on the regional winds (patterns) and population and emission sources distributions due to the topographic features. It makes sense for regional emissions mitigation policies.

Response: The wind speed and wind direction close related with the topography in the North China Plain has important impacts on the distribution of haze and fog. The aim of this paper is to discuss the wind field pattern, the attribution of particles transportation from Hebei Province on the haze pollution level in Beijing during a severe haze episode.

Local topographic certainly has important impacts on the meteorology fields including wind, this certainly may influence haze event and pollution level. But this is very complex and it is not possible to be discussed clearly as part content considering the length of this paper. Fu et al (2014) has ever discussed this in detail (Fu. et al., 2014). Anyway, we will pay much more attention on this in the following study on the whole winter of 2013-2014.

Fu, G. Q., Xu, W. Y., Yang, R. F., Li, J. B., and Zhao, C. S.: The distribution and trends of fog and haze in the North China Plain over the past 30 years. Atmospheric Chemistry and Physics, *14*(21), 11949-11958, doi: 10.5194/acp-14-11949-2014, 2014.

Minor comments

1. Line 8 on Page 3747: "..., and it changes the climate on a regional ..." may be changed into ". . ., it also has climate change effect over a regional . . ."

Response: It is revised in the manuscript.

2. Line 15 on Page 3747: "the central-eastern China, is not one of China's . . ." should be "the central-eastern China, is not only one of China's . . ."

Response: It is revised in the manuscript.

3. Line 21-22 on Page 3747: ". . . to inform policy aimed at averting irreversible environ- mental . . ." might be ". . . to inform policy aimed at averting environmental degradation ..."

Response: It is revised in the manuscript.

4. Line 3-4 on Page 3749: ". . . as a unified chemistry model . . ." could be changed into ". . . as a unified chemistry module . . ."

Response: It is revised in the manuscript.

5. Line 8-9 on Page 3749: You may remove “with diameter ranges of . . .. 20.48-40.96 μm” because the size bins have been defined in Gong’s paper (Gong, 2003) you cited.

Response: It is revised in the manuscript.

6. Line 21-22 on Page 3750: “Simulated PM2.5 values were similar to the observed PM2.5 values . . .” can be changed into “The simulated PM2.5 concentrations are in good agreement with observations...”

Response: It is revised in the manuscript.

7. What does “weather phenomena” mean in the manuscript? (Line 11 and 18 on Page 3751, Line 19 on Page 3757, and in Figure 2 caption). Weather phenomena can be any weather conditions that may and may not be hazardous to human life and property according to my understanding.

Response: It should be “haze weather phenomena” and this has been revised in the manuscript.

8. Line 17-20 on Page 3751: For high simulated PM2.5 in the southeastern Shanxi Province, please provide more evidences or detail explanations of “overestimated emissions”.

Response: The simulated PM2.5 has been on reasonable level after using the 2010 inventory, this figure is redrawn and the results using 2010 inventory are used in the manuscript.

9. Line 8 on Page 3758: "... 80 hPa ..." should be " ... 800 hPa ..."

Response: It is revised in the manuscript.

10. It is much better to develop a single figure to show the difference between mean observed and modeled visibility for 6-7 December 2013 instead of Figure 3 (a) and (b).

Response: Figure 3 has been redrawn.

11. Please improve the quality of Figure 4 because it is difficult to read numbers and legends with its normal size.

Response: Figure 4 has been redrawn.

Anonymous Referee #2

Technical comments:

1. Section 2.2: You wrote "The simulation period was 1-31 December 2013. The time step was set to 300 s, the forecasting time was 48 h, and the simulation began at 00:00 UTC every day". As I understand, your model simulation was re-initialized everyday at 00:00 UTC time, based on NCEP reanalysis data, and then run for 48 hours. That means you have one day's overlap for each run.

Probably, your description is not clear or even misleading. Therefore, my questions is, Do you really run your model like this? Or you re-initialized it every day, or using spin-up technique to restart it every day or every other day?

Response: Yes, We run the model at 00:00 UTC time everyday, based on NCEP reanalysis data and the chemical tracer initial field, and the simulation time is 48 hour. The monthly mean values of all tracers from observation data are used for initialization at the very beginning of the model run. The initial values of all gases in RADM2 and aerosol concentrations are based on the 24 h forecast made by the previous day's model run. The simulation results from 00 to 24 hours are used in this study. The model simulation begins from November 26 and the results of December 1-31 are used in order to avoid the uncertainties from the initial chemical fields at the model start. The brief explanation about this is added in the manuscript.

2. Section 3: You mentioned that SMOKE was used to transform your emission data into hourly gridded data require by GRAPES_CUACE model. SMOKE must know what chemical mechanism will be used in the air quality model (AQM) for which the SMOKE output emissions are intended. Here comes my

concerns: Do you use modified SMOKE version and did format transformation of emission data? If you use non- modified SMOKE, please give clear information, such as (a) What kind of chemical mechanism used by GRAPES_CUACE? and (2) how many chemical species involved in GRAPES_CUACE?

Response: Yes, we used modified SMOKE according to GRAPES_CUACE, which is similar to RADM II chemical mechanism. The detailed introduction of chemical species and chemical mechanism were given in the several papers (Gong and Zhang, 2008; Wang et al., 2015a, acp). The brief explanation and the related papers are also added in the manuscript and references.

3. Section 4.3: the formulas of Tans for four directions show that you divide Z direction in seven layers from ground to 3000m, what's exactly of this definition? Can you give some explanation in your text, and why you define like that? Base on what? Aerosol and/or dust transport layers, wind speed or some other reasons? Also, how did you define your grid cell distance dX, and dY for Beijing area? Based on your simulation domain grid resolution (0.25° x 0.25°) or some other conditions?

Response: The observation studies of haze events in east China (Wang et al., 2014a) showed "there is an aerosol extinction layer from the height of 1-1.5 km to 2-3 km from the ground, indicating most of the PM10 pollutants are mainly concentrated in the near ground atmosphere layer below 1 km and a small part of pollutants can also spread to the height of more than 2-3 km from the ground". The explanation about this and the related paper are also added in the manuscript and references

The grid cell distance dx and dy is based on simulation domain grid resolution (0.25° x 0.25°).

Minor comments:

4. Would you mind to add Local Time (LT) to Table 1? Readers have to convert all UTC time when they read your paper. I even suggest you convert all UTC times in your report to Local Time (LT), because your study focused on PM2.5 transport across cities in a small region area, readers will easily catch the time when the haze episode(s) happened at local time.

Response: The LT has been added after all the UTC times in the manuscript.

5. As I understand, all measurements are local time (Beijing time), and all model outputs are UTC time, but you did not mention that in your text. Please confirm that you converted time to same standard time during comparison.

Response: It was confirmed that they are all UTC time.

6. I find word “ca.” (no quotes) shows up in your paper many time, (e.g., Line 8 and 23 on page 3746, “at ca. 900 hPa” and “by ca. 10% per annum”) . Please check them in detail to see if this caused by font that you selected in your word document. I guess the meaning of “ca.” is about or “~”.

Response: Yes, “ca.” means circa (about) ， all “ca.” are replaced with “about” in the manuscript.

7. Line 23 on page 3747: “ as they are an important component ...”, probably should be changed to “as they are important components ...”

Response: It is revised in the manuscript.

8. Please avoid starting sentences with abbreviation that people not familiar with. For example, Line 16 on page 3752: “PK is currently experiencing...” should be : “Beijing is currently experiencing...”. Similar sentences at line 1-5 on page 3751 should also to be revised. I also noticed that you use “PK” instead of “BJ” as the abbreviation of “Beijing” in your whole paper, why not use “BJ”, although I know the reason.

Response: These are all revised in the manuscript. All “PK” are replaced with “BJ”

9. Please improve quality of figures 4, 6, 8 and 9. It's very hard to read them clearly even I zoomed them in five times on my screen. I suggest that your use bigger font size for axis labels and graph legends.

Response: The figures have been redrawn.

10. It's not easy to find the "close correlation" (line 7 on page 3752) from Figure 4. would you mind to create a supplementary panel plot including scatter plot with regression line for each comparison. Readers will catch how close correlation between model results and measurements.

Response: Figure 4 has been redrawn.

31 points are too few to make good scatter plot with regression line, so I added the regional average $PM_{2.5}$ of the whole Jing-Jin-Ji region to make it easier to find the close correlation.

11. Lines 24-26 on page 3750: please list station names in dictionary order, which can help readers track text and figures much more easier.

Response: It is revised in the manuscript.

12. Line 8-10 on page 3757: "As the calculation results in Table 1 show, ... by ca. 2727t from...". How did you get the value 2727t from Table 1, please explain it.

Response: The value 2727t was got from Fig.9. The total PM2.5 suspended over the PK area increased by about 2727 t from 12:00 UTC 6 December(980t) to 12:00 UTC 7 December (3707t). The explanation is also added in the manuscript.

Modeling study of $PM_{2.5}$ pollutant transport across cities in China's Jing–Jin–Ji region during a severe haze episode in December 2013

C. Jiang[1*], H. Wang[2*], T. Zhao[1], T. Li[1], H. Che[2]

1 Nanjing University of Information Science & Technology, Nanjing 210044, China
2 Institute of Atmospheric Composition, Chinese Academy of Meteorological Sciences (CAMS), CMA, Beijing, 100081, China

Corresponding author: C.Jiang (jc452@163.com) and H. Wang(wangh@cams.cma.gov.cn)

Abstract

To study the influence of particulate matter (PM) transported from surrounding regions on the high $PM_{2.5}$ pollution levels in Beijing, the GRAPES-CUACE model was used to simulate a serious haze episode that occurred on 6–7 December 2013. The results demonstrate the model's suitability for describing haze episodes throughout China, especially in the Beijing–Tianjin–Hebei (Jing–Jin–Ji) region. A very close positive correlation was found between the southerly wind speed over the plain to the south of Beijing and changes in $PM_{2.5}$ in Beijing, both reaching maximum values at about 900 hPa, suggesting the lower atmosphere was the principal layer for pollutant PM transport from its southern neighboring region to Beijing. During haze episodes, and dependent upon the period, Beijing was either a pollution source or sink for its surrounding area. PM input from Beijing's environs was much higher than the output from the city, resulting in the most serious pollution episode, with the highest $PM_{2.5}$ values occurring from 0000 to 1000 UTC(0800 to 1800 LT) 7 December 2013. PM pollutants from the environs of the city accounted for over 50% of the maximum $PM_{2.5}$ values reached in Beijing. At other times, the Beijing area was a net contributor to pollution in its environs.

删除的内容: ca.

1. Introduction

Air pollution has become a serious problem in megacities around the world (*Kanakidou et al., 2011*), and the topic has been receiving increased attention because of the close relationship between air pollution and the atmospheric environment, human health and ecosystems (*Kan et al., 2012; Liu et al., 2012*). China's air pollution has become increasingly serious since the economic reforms of 1978, which allowed rapid economic development. Gross Domestic Product has grown by about 10% per annum (*China Statistical Yearbook 2012, 2013*). China is now considered as one of the engines of global economic growth, but this rapid growth has resulted in an increase in energy consumption, air pollution, and associated health effects (*Chan et al., 2008*).

删除的内容: ca.

In recent years, haze has become a major pollution problem in Chinese cities (*Wu et al., 2010; Du et al., 2011; Tan et al., 2011*). Under the observation standards released by the China Meteorological Administration (CMA), haze is defined as a pollution phenomenon characterized by deteriorated horizontal visibility of <10 km, caused by fine particulate matter (PM) suspended in the atmosphere (*CMA, 2003*). Haze occurs when sunlight is absorbed and scattered by high concentrations of atmospheric aerosols (*E. Kang et al., 2013; Salinas et al., 2013*). It has a negative impact on human health and the environment (*Wu et al., 2005; Gurjar et al., 2010*), and it also has climate change effect over a regional or global scale by altering solar and infrared radiation in the atmosphere (*Wang et al., 2011; Yu et al., 2011; Chen et al., 2012*).

删除的内容: it changes the climate on

With an increasing number of local and regional haze events reported by the media, much attention has been paid to reducing air pollutant emissions and to improving air quality across the cities (*Huang et al., 2013; H. Kang et* al., 2013; Xu et al., 2013; Tan et al., 2014*), municipalities, and provinces of China (*Cheng et al., 2014; Ji et al., 2014*). The Jing–Jin–Ji region, located in central-eastern China, is not only one of China's most economically developed and industrialized regions, but is the area that most frequently experiences haze episodes (*Ji et al., 2014; H. Wang, S.-C. Tan, et al., 2014; L. T. Wang et al., 2014*). Beijing, at the center of the Jing–Jin–Ji region, is one of China's most economically developed cities, and has suffered from increasingly severe haze events (*Duan et al., 2012; Wang et al., 2012; Liu et al., 2014; Quan et al., 2014*). It is vital that air pollution in Beijing is studied in detail so as to inform policy aimed at averting irreversible environmental damage (*Cheng et al., 2013; Zhang et al., 2014*). The other areas of the Jing–Jin–Ji region should also be studied, as they are important components of the wider region and affect Beijing directly via the transport of PM pollutants (*Fu et al., 2014; Ying et al., 2014*). In the present reported study, an online mesoscale haze forecasting model was used to study the transport of major air pollutants to and from Beijing and the other areas of the Jing–Jin–Ji region (*Wang et al., 2013*).

删除的内容: an

2. Modeling

2.1 Model description

The new-generation Global/Regional Assimilation and PrEdiction System (GRAPES_Meso) and the Chinese Unified Atmospheric Chemistry Environment (CUACE) model developed by the Chinese Academy of Meteorological Science (CAMS), the CMA, were integrated to build an online chemical weather forecasting model, GRAPES-CUACE, focusing especially on haze pollution forecasting in China and East Asia (*Zhang et al., 2008; Wang et al., 2009*). GRAPES_Meso was adopted as the numerical weather prediction model for aerosol determination. It is a new-generation general hydrostatic/non-hydrostatic, multi-scale numerical model developed by the

Research Center for Numerical Meteorological Prediction, CAMS, CMA (*Zhang* and *Shen, 2008*). The model uses standardized and module-based software and has been developed in accordance with strict software engineering requirements, including program-operated parallel calculations (*Xue et al., 2008*). Testing has shown that the design and application of the model meet these prerequisites, and that it can therefore serve as a good foundation for the sustainable development of a numerical prediction system for China (*Chen et al., 2008*). The large-scale horizontal and vertical transportation and diffusion processes for all gases and aerosols can also be processed using GRAPES_Meso's dynamic framework (*Xu et al., 2008*). Again, testing has demonstrated that both the design of the model's framework and its implementation meet the requirements of real-time operational weather forecasting, especially in China and East Asia. GRAPES_Meso has therefore been used as an operational, real-time, short-term weather prediction system in China since 2009 (*Yang et al., 2008; Zhu et al., 2008*).

The CUACE model was developed by the CAMS Centre for Atmosphere Watch And Services (CAWAS). It is a newly developed system for testing and forecasting air quality in China that includes four functions: treating aerosols; gas phase chemistry; emissions; and data assimilation (*Gong* *and Zhang*, *2008*). The detailed data capture by this model of processes such as aerosol sources, transport, dry and wet deposition, and dust removal both in and below clouds, clearly describes the interaction between aerosols and clouds (*Zhou et al., 2008*). CUACE has been designed as a unified chemistry module that can be easily coupled with any atmospheric model (e.g. regional air quality and climate models) at various temporal and spatial scales. It has thus been integrated online with GRAPES_Meso to produce the GRAPES-CUACE model (*Wang et al., 2009,2010,2014c*). Dust particles are divided into 12 size bins (*Gong, 2003*), following guidelines provided by the measurement of soil

删除的内容: &

删除的内容: *et al.*

删除的内容: model

删除的内容: with diameter ranges of 0.01–0.02, 0.02–0.04, 0.04–0.08, 0.08–0.16, 0.16–0.32, 0.32–0.64, 0.64–1.28, 1.28–2.56, 2.56–5.12, 5.12–10.24, 10.24–20.48 and 20.48–40.96 μm dust size in Chinese desert regions during 1994–2001(*Zhang, 2003*).

2.2 Model domain and parameters

In this study, GRAPES-CUACE was used to simulate a haze episode in December 2013. The model's vertical cap was set at about 30 km, with 31 vertical layers. As shown in Figure 1, its domain covered the East Asia region (20°–55°N, 90°–140°E) with a horizontal resolution of 0.25° × 0.25°. National Centers for Environmental Prediction (NCEP) 1° × 1° reanalysis data were used for the model's initial and six-hour meteorological lateral direction input fields. The model ran at 0000 UTC time everyday, based on NCEP reanalysis data and the chemical tracer initial field, and the simulation time is 48 hour. The monthly mean values of all tracers from observation data are used for initialization at the very beginning of the model run. The initial values of all gases in RADM2 and aerosol concentrations are based on the 24 h forecast made by the previous day's model run. The simulation results from 00 to 24 hours are used in this study. The model simulation begins from November 26 and the results of December 1-31 are used in order to avoid the uncertainties from the initial chemical fields at the model start.

删除的内容: ca.

删除的内容: The simulation period was 1–31 December 2013. The time step was set to 300 s, the forecasting time was 48 h, and the simulation began at 0000 UTC every day.

3. Data description

This study employed CMA ground visibility and operational weather observation data. The data covered mainland China, including a total of 600 ground observation stations.

The daily mean $PM_{2.5}$ concentrations were from surface observations made by the China National Environmental Monitoring Center (CNEMC, http://www.cnpm25.com). They included values for 74 cities in mainland China. The data represented the mean values of data from different observation stations distributed in various downtown, suburb, and suburban areas of each city. For example, pollutant concentrations in Beijing were obtained by extracting the mean value from the data from 12 observation sites. This value was then used to represent the mean pollution conditions for each city as a whole.

Detailed high-resolution emission inventories of reactive gases from emissions over China in 2007, i.e. for SO_2, NO_x, CO, NH_3, and volatile organic compounds (VOCs), were updated to form current emission data, based on official national emission source criteria *(Cao et al., 2006; 2010)*. The Sparse Matrix Operator Kernel Emissions (SMOKE) system was used to transform these emission data into the hourly-gridded data required by the GRAPES_CUACE model, including the five aerosol species of black carbon (BC), organic carbon (OC), sulfate, nitrate, and fugitive dust particles, in addition to 27 gases, such as VOCs, NH_3, CO, CO_2, SO_x and NO_X *(An et al., 2013)*. Modified SMOKE was used according to GRAPES_CUACE, which is similar to RADM II chemical mechanism. The detailed introduction of chemical species and chemical mechanism were given in the several papers (*Gong and Zhang, 2008; Wang et al., 2015*).

4. Results

4.1 Model evaluation

First, the simulation results were compared with the observation data from the major cities in the Jing–Jin–Ji region during the haze episode of 6–7 December to evaluate the model's capabilities. The Jing-Jin-Ji region and the Yangtze River Delta (YRD) region were the most severely polluted during 6–7 December, with mean observed $PM_{2.5}$ values for the two-day period of about 200 μg/m^3 (Fig. 1). The simulated PM2.5 concentrations are in good agreement with observations for most of the cities, especially in the Jing–Jin–Ji region (e.g. Baoding (BD), Beijing (BJ), Cangzhou (CZ), Chengde (CD), Dezhou (DZ), Jinan (JN), Handan (HD), Hengshui (HS), Qinhuangdao (QHD),

带格式的： 字体:斜体

删除的内容: ca.

删除的内容: Simulated $PM_{2.5}$ values were similar to the observed $PM_{2.5}$ values

删除的内容: Zhangjiakou (ZJK), Chengde (CD), Qinhuangdao (QHD), Beijing (PK), Tianjin (TJ), Baoding (BD), Cangzhou (CZ), Shijiazhuang (SJZ), Hengshui (HS), Xingtai (XT), Handan (HD), Dezhou (DZ) and Jinan (JN)

Shijiazhuang (SJZ), Tianjin (TJ), Xingtai (XT) and Zhangjiakou (ZJK)). Both datasets showed that cities in the northern Jing–Jin–Ji region experienced lower levels of pollution and were less affected by $PM_{2.5}$ during this haze episode (e.g. ZJK, CD, and QHD, with observed $PM_{2.5}$ concentrations of 59.1, 51.9 and 94.1 μg/m^3, respectively, and simulated $PM_{2.5}$ concentrations of 30.9, 44.3 and 60.1 μg/m^3, respectively), while the cities in the central and southern sectors of the Jing–Jin–Ji region experienced severe pollution and high $PM_{2.5}$ levels (e.g. BJ, TJ, BD, CZ, SJZ, HS, XT, HD, DZ and JN, with observed $PM_{2.5}$ concentrations of 194.3, 165.6, 302.1, 237.3, 268.7, 160.1, 295.1, 223.3, 224.3 and 149.9 μg/m^3, respectively, and simulated $PM_{2.5}$ concentrations of 115.7, 207.1, 250.1, 267.0, 237.7, 326.5, 323.3, 263.6, 312.1 and 256.1 μg/m^3, respectively). The modeled results thus accurately described the haze episode over the whole region.

The horizontal distribution of simulated $PM_{2.5}$ concentrations was compared with observed haze weather phenomena in eastern China. The centralized hazy weather observed in the region at 1400 UTC(2200 LT) 7 December 2013 corresponded with the area of high simulated $PM_{2.5}$ (Fig. 2). Simulated $PM_{2.5}$ values were >150 μg/m^3 for the whole of eastern China, with most areas of the highest concentration reaching 300 μg/m^3 or even 500 μg/m^3. Hazy weather was concentrated in the Jing–Jin–Ji region, i.e. Shandong, Jiangsu, and Zhejiang provinces, and Shanghai. There were clearly delineated areas of high simulated $PM_{2.5}$ values that corresponded with these regions.

There was an obvious demarcation line with respect to observed visibility from the southwest to the northeast, dividing China into high visibility and low visibility regions, with the low visibility region centered on the YRD (Fig. 3). The simulated visibility showed similar results (Fig. 3), albeit it was lower than the observed visibility in Shandong, southern Hebei and Shanxi provinces.

删除的内容: PK

删除的内容: However, high simulated $PM_{2.5}$ values did not match the observed $PM_{2.5}$ and weather phenomena for southeastern Shanxi Province, which may be because emissions were overestimated in the 2007 inventory. Simulated results will improve further once the 2010 inventory can be used.

删除的内容: a

删除的内容: b

Several major cities, including BJ, BD, CZ, DZ, HD, HS, SJZ, XT and Zhengzhou (ZZ) in the Jing–Jin–Ji region and its environs, and Shanghai (SH) and Nanjing (NJ) in the YRD, were selected for a comparison of daily average observed and simulated $PM_{2.5}$ values during 1–31 December 2013, to test the validity of long-term simulations. As shown in Figure 4, the simulated daily results were fairly close to the observed values for the 6–7 December haze episode. Beginning on 6 December, this episode was most severe on 7 December; and then $PM_{2.5}$ levels decreased rapidly from 8 December onwards. The simulated results for Beijing and the average of whole Jing-Jin-Ji region were highly consistent with the trends in observed daily values for the whole of December. Simulated results for the other cities in the Jing–Jin–Ji region also showed close correlation with observed data for 6–7 December, even considering that the maximum value appeared one day earlier in HS and one day later in SH. While the simulated values for NJ were lower than the observed data, they essentially exhibited the same daily trends.

删除的内容: PK, HD, SJZ, BD, XT, HS, DZ

The results obtained by GRAPES-CUACE for the Jing–Jin–Ji region through its simulation of $PM_{2.5}$ concentrations demonstrate the model's suitability for studying the impact of particulate transport on $PM_{2.5}$ concentrations. The Jing–Jin–Ji region was therefore chosen as an appropriate study area.

4.2 Wind field

Beijing is currently experiencing the severest haze pollution in its history. On the plains of Hebei to the south, the most seriously polluted area in China, haze and fog episodes are much more serious even than in Beijing. Seven of the 10 cities with the highest levels of $PM_{2.5}$ pollution in China are located in this region (*Wang et al., 2014a, 2014b*). The contribution made by cross-city pollutants transported from southern Hebei Province to levels of $PM_{2.5}$ pollution in BJ is receiving much attention. The construction of the wind field

删除的内容: PK

删除的内容: PK

over this region, particularly the wind field pattern in the planetary boundary layer (PBL), is a key factor in determining the impact of the cross-city transport of $PM_{2.5}$ pollutants.

The wind field was analyzed to study the impact that PM transport from its environs had on air pollution in BJ during the haze episode of the present study. As Figure 5a shows, $PM_{2.5}$ concentrations in BJ reached their maximum at 0800 UTC(1600 LT) 7 December. Stable southwesterly winds affected BJ and the area to the south of BJ, while the wind direction was northwesterly and the wind speed lower in the region to the north of BJ. From both the observed and simulated data (Figs. 1, 2, and 3), it is apparent that the region to the south of BJ was the most polluted area, with the highest $PM_{2.5}$, lowest visibility and densest haze, and this region was therefore the likely main contributor to pollution levels in BJ during this haze episode. The vertical section along 115.25°E (Fig. 5b) enabled us to explore the relationship between the wind field and $PM_{2.5}$ concentrations and transport at different vertical heights. Figure 5b shows a southwesterly wind at 39°N blowing from the surface to the 800 hPa level in the region's southern sector. In the southern sector closest to BJ, the southerly wind speed reached its maximum value at about 900 hPa; and $PM_{2.5}$ also exhibited high values at the same height. Pollutants could thus be transported to BJ by the stable southwesterly wind from the southern environs via the 900 hPa layer. The northerly, or very weak southerly, wind in the region north of 41°N, together with the southerly wind south of 39°N, led to the formation of a wind convergence field over BJ stretching from the surface level to 900 hPa. This would have been beneficial to the accumulation of $PM_{2.5}$ and the consequent aggravation of haze. The vertical section along 39.375°N describes a southerly wind in the region to the south of BJ from 116°E to 125°E (Fig. 5c). This southerly wind, extending from the surface to 800 hPa, reached its maximum velocity at 900 hPa in the area to the south of BJ (116°E to 118°E). $PM_{2.5}$ concentrations were also

删除的内容: PK
删除的内容: PK
删除的内容: PK
删除的内容: PK
删除的内容: PK
删除的内容: PK
删除的内容: PK
删除的内容: PK
删除的内容: ca.
删除的内容: PK
删除的内容: PK
删除的内容: PK
删除的内容: PK

significantly higher in this region; pollutants from the 116°–125°E area would have been easily transported northward by the southerly wind. BJ was most likely affected by this process, raising pollution levels and aggravating the haze.

删除的内容: PK

To verify these results, we analyzed the relationship between $PM_{2.5}$ concentrations in BJ and the wind field of the area to the south of BJ (i.e. 113.5°–118°E, 34.5°–39.5°N) (Fig. 5a). In the analysis, positive average hourly wind speed (*v*) values were representative of a southerly wind, and negative *v* values a northerly wind. The results showed that, when there was southerly wind in the area to the south of BJ, average $PM_{2.5}$ concentrations in BJ always increased (Fig. 6). This was most obvious on 7 December, when the highest $PM_{2.5}$ values occurred, accompanied by longer periods of stable southerly winds. When there was a northerly wind in the area to the south of BJ, average $PM_{2.5}$ concentrations in BJ fell, and then stabilized.

删除的内容: PK

删除的内容: PK

删除的内容: PK

删除的内容: PK

删除的内容: PK

删除的内容: PK

4.3 BJ's $PM_{2.5}$ input and output

删除的内容: PK

To investigate the contribution of $PM_{2.5}$ transported from its surroundings to BJ pollution levels, the transport rates (kg/s) for $PM_{2.5}$ from four directions, east (E), west (W), south (S) and north (N), were calculated using the following formulas:

删除的内容: PK

$$Tran_N(t) = \sum_{z=1}^{7} \sum_{x=x_1}^{x_2} PM_{y_1}(x,z,t) \cdot \Delta x_{y_1} \cdot \Delta z_{y_1}(x,z) \cdot v_{y_1}(x,z,t)$$

$$Tran_N(t) = \sum_{z=1}^{7} \sum_{x=x_1}^{x_2} PM_{y_1}(x,z,t) \cdot \Delta x_{y_1} \cdot \Delta z_{y_1}(x,z) \cdot v_{y_1}(x,z,t)$$

$$Tran_N(t) = \sum_{z=1}^{7} \sum_{x=x_1}^{x_2} PM_{y_1}(x,z,t) \cdot \Delta x_{y_1} \cdot \Delta z_{y_1}(x,z) \cdot v_{y_1}(x,z,t)$$

$$Tran_N(t) = \sum_{z=1}^{7} \sum_{x=x_1}^{x_2} PM_{y_1}(x,z,t) \cdot \Delta x_{y_1} \cdot \Delta z_{y_1}(x,z) \cdot v_{y_1}(x,z,t)$$

$$Tran_N(t) = \sum_{z=1}^{7} \sum_{x=x_1}^{x_2} PM_{y_1}(x,z,t) \cdot \Delta x_{y_1} \cdot \Delta z_{y_1}(x,z) \cdot v_{y_1}(x,z,t)$$

where $Tran_N$, $Tran_S$, $Tran_E$ and $Tran_W$ represent the $PM_{2.5}$ transport rate for N, S, E and W, respectively (Fig. 7). Positive *Tran* values indicated net pollutant input into BJ; negative *Tran* values described net pollutant output from BJ. PM stands for $PM_{2.5}$ concentration; x_1, x_2 (Fig. 7) are the westernmost and easternmost BJ longitudes, respectively, and the subscripts y_1, y_2 (Fig. 7) are the southernmost and northernmost BJ latitudes; *t* stands for time; Δ*x*, Δ*y*, Δ*z* indicate the individual grid distances of the *x*, *y*, *z* axes; *u* stands for the easterly/westerly wind speed (negative for easterly wind); and *v* stands for the southerly/northerly wind speed (negative for northerly wind). The constantly negative $PM_{2.5}$ transport rate toward BJ, reaching a maximum rate of −112.8 kg/s at 1100 UTC(1900 LT) in the southerly direction, indicated a constant output of $PM_{2.5}$ southward from BJ to its southern environs on 6 December (Fig. 8a). Eastward $PM_{2.5}$ transport rates were largely negative before 1200 UTC(2000 LT), indicating net $PM_{2.5}$ output from BJ downwind. After 1200 UTC(2000 LT), the $PM_{2.5}$ transport rate became slightly positive and then remained steady, indicating a small net input in the afternoon. There was little westerly or northerly transport throughout the day.

The total input/output rate was calculated by summing the input/output transport rate for the four directions; and the net transport rate was obtained by summing the total input and output rate. Positive net transport values indicated that the BJ area was receiving $PM_{2.5}$ from its surroundings; negative net values showed BJ to be exporting $PM_{2.5}$ to its surroundings. The total output rate clearly exceeded the input rate, and the net transport rate was negative, indicating a net output of pollutants from BJ during the period 0000–

删除的内容: PK
删除的内容: PK
删除的内容: PK
删除的内容: PK
删除的内容: PK
删除的内容: PK
删除的内容: PK
删除的内容: PK
删除的内容: PK
删除的内容: PK

1300 UTC(0800-2100 LT) 6 December (Fig. 8b). After 1400 UTC(2200 LT), the output rate clearly fell, while the input rate remained substantially unchanged, resulting in the net transport rate falling close to zero. This shows that the BJ area was a source of pollutants for the areas to its east and south throughout the whole of 6 December.

For 7 December (the most polluted day in this episode), transport rate values for each direction changed substantially (Fig. 8c). There were large positive values for westerly and southerly winds, indicating major $PM_{2.5}$ transport from these directions to BJ; and this correlates with the inferences drawn from Figure 5 and Figure 6. The transport rate eastward was always positive, reaching a maximum of 149.5 kg/s at 0800 UTC(1600 LT); it was always negative in the westward direction, reaching a minimum of −174.2 kg/s at 1200 UTC(2000 LT). This suggests that a westerly wind dominated on 7 December and transported $PM_{2.5}$ from the area to the west of BJ to the city and to its eastern downwind area. $PM_{2.5}$ transport was heaviest at 0800 UTC(1600 LT) and 1200 UTC(2000 LT) from the west and east, respectively. There was input from the south and output northward before 1100 UTC(1900 LT), with concurrent maxima of 86.4 and 22.6 kg/s at 0800 UTC(1600 LT), respectively. After 1200 UTC(2000 LT), the wind direction became northerly, leading to a reversal in the direction of input/output pollutant transport. Net pollutant output turned southward; the output rate was clearly greater than the input rate from the north during the period 1200–2400 UTC 7 December(2000 LT 7 December to 0800 LT 8 December).

The net transport rate for BJ on 7 December was positive before 1000 UTC(1800 LT), rising from about zero to a maximum of 118.1 kg/s at 0600 UTC(1400 LT), and then began to decline to consistently negative values after 1100 UTC(1900 LT) (Fig. 8d). This suggests that the input of pollutants into BJ exceeded the output during the period 0000–1000 UTC(0800-1800 LT).

删除的内容: PK

删除的内容: PK

删除的内容: PK

删除的内容: PK

删除的内容: ca.

删除的内容: PK

After 1100 UTC(1900 LT), input transport rates into BJ were markedly reduced, resulting in a net negative transport of pollutants, indicating that BJ was a source of pollutants for its environs. Combined with the results from Figure 8c, there was net pollutant output to BJ's east and south. By analyzing Figure 8c and Figure 8d, it can be seen that changes in the net transport rate for BJ correlated with the transport rate southward. This was principally because westerly input and easterly output were basically equal and so offset one another. The northward transport rate was consistently low, and the variable southward transport rate therefore had an enormous influence on the BJ area. These results indicate that pollutant transport between BJ and its southern environs had the most significant impact on pollution levels in BJ in comparison to other areas.

4.4 Contribution of pollutant transport to $PM_{2.5}$ concentrations over BJ

The observation studies of haze events in east China (Wang et al., 2014a) showed "there is an aerosol extinction layer from the height of 1-1.5 km to 2-3 km from the ground, indicating most of the PM10 pollutants are mainly concentrated in the near ground atmosphere layer below 1 km and a small part of pollutants can also spread to the height of more than 2-3 km from the ground". In order to evaluate the contribution made by pollutants transported from its environs to BJ $PM_{2.5}$ pollution, the total $PM_{2.5}$ suspended in the atmosphere between the surface and a height of 3000 m over the BJ area during this haze episode was calculated, according to the formula

$$Tran_N(t) = \sum_{z=1}^{7} \sum_{x=x_1}^{x_2} PM_{y_1}(x,z,t) \cdot \Delta x_{y_1} \cdot \Delta z_{y_1}(x,z) \cdot v_{y_1}(x,z,t),$$

along with the net hourly transport amount (Fig. 9). Total $PM_{2.5}$ changed little during 6 December, but did rise slightly after a small decline at 1200

删除的内容: PK
删除的内容: PK
删除的内容: PK
删除的内容: PK
删除的内容: PK
删除的内容: PK
删除的内容: PK
删除的内容: **PK**
删除的内容: PK
删除的内容: PK

UTC(2000 LT) when the net hourly output transport value decreased. The total $PM_{2.5}$ amount continued rising on 7 December and began to accelerate sharply until 0900 UTC(1700 LT) (4555.4 t) with a large net hourly input. After 1200 UTC(2000 LT), net hourly transport became highly negative, and total $PM_{2.5}$ decreased rapidly. By the end of 7 December, the total $PM_{2.5}$ suspended in the atmosphere over BJ was consistent with the values for 6 December. As Figure 9 shows, this sharp rise in total $PM_{2.5}$ began at 1200 UTC(2000 LT) on 6 December(980t), and ended at 1200 UTC(2000 LT) on 7 December(3707t), when total $PM_{2.5}$ reached its maximum value before beginning to decrease, and, the total $PM_{2.5}$ suspended over the BJ area increased by about 2727 t in this period. As the calculation results in Table 1 show, net input was 1497 t, accounting for 55% of the total $PM_{2.5}$ increase(2727t) from 1200 UTC(2000 LT) 6 December to 1200 UTC(2000 LT) 7 December. The remaining 1230 t could be attributed to local effects, and accounted for 45% of the total $PM_{2.5}$ increase (Fig. 10). This suggests that the transport of particle pollutants from its environs made a significant contribution to the peak $PM_{2.5}$ values over BJ during this haze episode.

删除的内容: PK

删除的内容: .

删除的内容: , the total $PM_{2.5}$ suspended over the PK area increased by ca. 2727 t from 1200 UTC 6 December to 1200 UTC 7 December. N

删除的内容: local emissions

删除的内容: PK

5. Conclusion

The GRAPES-CUACE online mesoscale chemical weather forecasting model was used to study the influence of PM transported from its near environs on high $PM_{2.5}$ pollution levels in BJ during a severe haze episode on 6–7 December 2013. Simulated results were compared with ground-level horizontal visibility, haze weather phenomena as observed by CMA, and surface $PM_{2.5}$ concentrations observed by CNEMC, to evaluate the model's ability to accurately describe haze pollution in China. The 3D wind field over the Jing–Jin–Ji region and its relationship with $PM_{2.5}$ variations in BJ, the input/output pollutant transport rates for BJ and its N, S, E and W environs, the total input, output and net pollutant transport amounts for BJ, and the total

删除的内容: PK

删除的内容: PK

删除的内容: PK

删除的内容: PK

$PM_{2.5}$ suspended in the atmosphere over BJ, were all calculated in relation to the possible contribution of $PM_{2.5}$ transported from its environs to the high $PM_{2.5}$ pollution levels in BJ during the aforementioned severe haze episode. The results can be summarized as follows:

(1) The spatial and temporal comparison of the simulated results with observational data showed that the model is capable of accurately describing haze episodes in China, and especially in the Jing–Jin–Ji region. This then formed a sound foundation for the calculation of PM transported across cities in this region.

(2) There was a very close positive correlation between the southerly wind speed over the area to the south of BJ and $PM_{2.5}$ variations in BJ, suggesting the likely important contribution made by PM transport from BJ's southern environs to the city. At 0800 UTC(1600 LT) on 7 December, southwesterlies from the surface to 800 hPa were largely stable in BJ and its southern environs; the region north of BJ was affected by a gentle wind. Both the southerly wind speed in the area to the south of BJ, and $PM_{2.5}$, reached their maxima at about 900 hPa, suggesting this height served as the major transport layer for pollutants from the south to BJ.

(3) The BJ area was a net output source for its environs for most of the haze episode during 6–7 December, except for the period from 0000 to 1000 UTC(0800 to 1800 LT) 7 December, when the haze was at its most serious and was accompanied by the highest $PM_{2.5}$ values. Input from the west was more or less offset by transport eastward. The input rate from the south was much higher than the output rate to the north from 0000 to 1000 UTC(0800 to 1800 LT) 7 December, and there was thus a net input during this period, resulting in the most serious pollution levels and peak $PM_{2.5}$ values for this haze episode. This shows that pollutant transport from the south was the major contributor to the peak $PM_{2.5}$ pollution levels in the BJ area.

删除的内容: PK
删除的内容: PK
带格式的
删除的内容: PK
删除的内容: PK
删除的内容: PK
删除的内容: PK
删除的内容: PK
删除的内容: PK
删除的内容: ca.
删除的内容: PK
删除的内容: PK
删除的内容: PK

(4) Total $PM_{2.5}$ suspended in the atmosphere from the surface to 3000 m over the BJ area changed very little during 6 December. Total $PM_{2.5}$ began to rise slightly at 1200 UTC(2000 LT) 6 December, when the net hourly output transport rate decreased; then rose clearly at 0000 UTC(0800 LT) 7 December; and was followed by a rising trend that maintained until 0900 UTC(1700 LT) 7 December, accompanied by high net hourly input values. After 1200 UTC(2000 LT), the net hourly transport rate became significantly negative as total $PM_{2.5}$ decreased rapidly. Total $PM_{2.5}$ suspended over BJ increased by about 2727 t from 1200 UTC(2000 LT) 6 December to 1200 UTC(2000 LT) 7 December. The total net input was 1497 t, accounting for 55% of the total $PM_{2.5}$ increase during this period. The remaining 1230 t could be attributed to local effects, and accounted for 45% of the total $PM_{2.5}$ increase. This suggests that PM transport from its environs significantly influenced the peak $PM_{2.5}$ values over BJ during this episode.

删除的内容: PK

删除的内容: PK

删除的内容: ca.

删除的内容: emissions

删除的内容: PK

Acknowledgements

This work was supported by the National Basic Research Program (973) (Grant No. 2014CB441201), the National Natural Scientific Foundation of China (Grant Nos. 41275007 & 41130104), the Jiangsu Collaborative Innovation Center for Climate Change， CAMS key projects (Grant No. 2013Z007), the Science and Technology Support Program of Jiangsu Province (Grant No. BE2012771), and the Priority Academic Program Development of Jiangsu Higher Education Institutions (PAPD).

References

An, X. Q., Sun, Z. B., Lin, W. l., Jin, M., and Li, N.: Emission inventory evaluation using observations of regional atmospheric background stations of China, J. Environ. Sci., 25, 537–546, 2013.

Cao, G., Zhang, X., and Zheng, F.: Inventory of black carbon and organic carbon 446 emissions from China, Atmos. Environ., 40, 6516–27, 2006.

Cao, G. L., AN, X. Q., Zhou, C. H., Ren, Y. Q., and Tu, J.: Emission inventory of air pollutants in China, Chin. Environ. Sci., 30, 900–906, 2010.

Chan, C. K. and Yao, X.: Air pollution in mega cities in China, Atmos. Environ., 42, 1–42, doi:10.1016/j.atmosenv.2007.09.003, 2008.**TS3**

Chen, D., Xue, J., Yang, X., Zhang, H., Shen, X., Hu, J., Wang, Y., Ji, L., and Chen, J.: New generation of multi-scale NWP system (GRAPES): general scientific design, Chinese Sci. Bull., 53, 3433–3445, doi:10.1007/s11434-008-0494-z, 2008.

Chen, Y., Liu, Q., Geng, F., Zhang, H., Cai, C., Xu, T., Ma, X., and Li, H.: Vertical distribution of optical and micro-physical properties of ambient aerosols during dry haze periods in Shanghai, Atmos. Environ., 50, 50–59, doi:10.1016/j.atmosenv.2012.01.002, 2012.

Cheng, Y., Engling, G., He, K.-B., Duan, F.-K., Ma, Y.-L., Du, Z.-Y., Liu, J.-M., Zheng, M., and Weber, R. J.: Biomass burning contribution to Beijing aerosol, Atmos. Chem. Phys., 13, 7765–7781, doi:10.5194/acp-13-7765-2013, 2013.

Cheng, Z., Wang, S., Fu, X., Watson, J. G., Jiang, J., Fu, Q., Chen, C., Xu, B., Yu, J., Chow, J. C., and Hao, J.: Impact of biomass burning on haze pollution in the Yangtze River delta, China: a case study in summer 2011, Atmos. Chem. Phys., 14, 4573–4585, doi:10.5194/acp-14- 4573-2014, 2014.

China Statistical Yearbook 2012, 2013, National Bureau of Statistics of China, China Statistics Press, Beijing, 2012, 2013.

CMA: Specifications for the Surface Meteorological Observations, Meteorological Press, Beijing, China (in Chinese), 2003.

Du, H., Kong, L., Cheng, T., Chen, J., Du, J., Li, L., Xia, X., Leng, C., and Huang, G.: Insights into summertime haze pollution events over Shanghai based on online water-soluble ionic com- position of aerosols, Atmos. Environ., 45, 5131–5137, doi:10.1016/j.atmosenv.2011.06.027, 2011.

Duan, J., Guo, S., Tan, J., Wang, S., and Chai, F.: Characteristics of atmospheric carbonyls during haze days in Beijing, China, Atmos. Res., 114–115, 17–27, doi: 10.1016/j.atmosres.2012.05.010, 2012.

Fu, X., Wang, S. X., Cheng, Z., Xing, J., Zhao, B., Wang, J. D., and Hao, J. M.: Source, transport and impacts of a heavy dust event in the Yangtze River Delta, China, in 2011, Atmos. Chem. Phys., 14, 1239–1254, doi:10.5194/acp-14-1239-2014, 2014.

Gong, S. L.: Characterization of soil dust aerosol in China and its transport and distribution during 2001 ACE-Asia: 2. Model simulation and validation, J. Geophys. Res., 108, doi:10.1029/2002jd002633, 2003.

Gong, S. L. and Zhang, X. Y.: CUACE/Dust – an integrated system of observation and modeling systems for operational dust forecasting in Asia, Atmos. Chem. Phys., 8, 2333–2340, doi:10.5194/acp-8-2333-2008, 2008.

Gurjar, B. R., Jain, A., Sharma, A., Agarwal, A., Gupta, P., Nagpure, A. S., and Lelieveld, J.: Human health risks in megacities due to air pollution, Atmos. Environ., 44, 4606–4613, doi:10.1016/j.atmosenv.2010.08.011, 2010.

Huang, K., Zhuang, G., Lin, Y., Wang, Q., Fu, J. S., Fu, Q., Liu, T., and Deng, C.: How to improve the air quality over megacities in China: pollution characterization and source analysis in Shanghai before, during, and after the 2010 World Expo, Atmos. Chem. Phys., 13, 5927– 5942, doi:10.5194/acp-13-5927-2013, 2013.

Ji, D., Li, L., Wang, Y., Zhang, J., Cheng, M., Sun, Y., Liu, Z., Wang, L., Tang, G., Hu, B., Chao, N., Wen, T., and Miao, H.: The heaviest particulate air-pollution episodes occurred in northern China in January, 2013: insights gained from observation, Atmos. Environ., 92, 546–556, doi:10.1016/j.atmosenv.2014.04.048, 2014.

Kan, H., Chen, R., and Tong, S.: Ambient air pollution, climate change, and population health in China, Environ Int., 42, 10–19, doi:10.1016/j.envint.2011.03.003, 2012.

Kanakidou, M., Mihalopoulos, N., Kindap, T., Im, U., Vrekoussis, M., Gerasopoulos, E., Der- mitzaki, E., Unal, A., Koçak, M., Markakis, K., Melas, D., Kouvarakis, G., Youssef, A. F., Richter, A., Hatzianastassiou, N., Hilboll, A., Ebojie, F., Wittrock, F., von Savigny, C., Burrows, J. P., Ladstaetter-Weissenmayer, A., and Moubasher, H.: Megacities as hot spots of air pollution in the East Mediterranean, Atmos. Environ., 45, 1223–1235, doi: 10.1016/j.atmosenv.2010.11.048, 2011.

Kang, E., Han, J., Lee, M., Lee, G., and Kim, J. C.: Chemical characteristics of size-resolved aerosols from Asian dust and haze episode in Seoul Metropolitan City, Atmos. Res., 127, 34–46, doi:10.1016/j.atmosres.2013.02.002, 2013.

Kang, H., Zhu, B., Su, J., Wang, H., Zhang, Q., and Wang, F.: Analysis of a long-lasting haze episode in Nanjing, China, Atmos. Res., 120–121, 78–87, doi: 10.1016/j.atmosres.2012.08.004, 2013.

Liu, Q., Liu, Y., Yin, J., Zhang, M., and Zhang, T.: Chemical characteristics and source apportionment of PM10 during Asian dust storm and non-dust storm days in Beijing, Atmos. Environ., 91, 85–94, doi:10.1016/j.atmosenv.2014.03.057, 2014.

Liu, W.-T., Hsieh, H.-C., Chen, S.-P., Chang, J. S., Lin, N.-H., Chang, C.-C., and Wang, J.-L.: Diagnosis of air quality through observation and modeling of volatile organic compounds (VOCs) as pollution tracers, Atmos. Environ., 55, 56–63, doi:10.1016/j.atmosenv.2012.03.017, 2012.

Quan, J., Tie, X., Zhang, Q., Liu, Q., Li, X., Gao, Y., and Zhao, D.: Characteristics of heavy aerosol pollution during the 2012–2013 winter in Beijing, China, Atmos. Environ., 88, 83–89,

doi:10.1016/j.atmosenv.2014.01.058, 2014.
Salinas, S. V., Chew, B. N., Miettinen, J., Campbell, J. R., Welton, E. J., Reid, J. S., Yu, L. E., and Liew, S. C.: Physical and optical characteristics of the October 2010 haze event over Singapore: a photometric and lidar analysis, Atmos. Res., 122, 555–570, doi:10.1016/j.atmosres.2012.05.021, 2013.
Tan, J., Guo, S., Ma, Y., Duan, J., Cheng, Y., He, K., and Yang, F.: Characteristics of particulate PAHs during a typical haze episode in Guangzhou, China, Atmos. Res., 102, 91–98, doi:10.1016/j.atmosres.2011.06.012, 2011.
Tan, J., Yang, L., Grimmond, C. S. B., Shi, J., Gu, W., Chang, Y., Hu, P., Sun, J., Ao, X., and Han, Z.: Urban integrated meteorological observations: practice and experience in Shanghai, China, B. Am. Meteorol. Soc., 140602092802009, doi:10.1175/bams-d-13-00216.1, 2014.
Wang, G., Chen, C., Li, J., Zhou, B., Xie, M., Hu, S., Kawamura, K., and Chen, Y.: Molecular composition and size distribution of sugars, sugar-alcohols and carboxylic acids in airborne particles during a severe urban haze event caused by wheat straw burning, Atmos. Environ., 45, 2473–2479, doi:10.1016/j.atmosenv.2011.02.045, 2011.
Wang, H., Gong, S., Zhang, H., Chen, Y., Shen, X., Chen, D., Xue, J., Shen, Y., Wu, X., and Jin, Z.: A new-generation sand and dust storm forecasting system GRAPES_CUACE/Dust: model development, verification and numerical simulation, Chinese Sci. Bull., 55, 635–649, doi:10.1007/s11434-009-0481-z, 2009.
Wang, H., Zhang, X., Gong, S., Chen, Y., Shi, G., and Li, W.: Radiative feedback of dust aerosols on the East Asian dust storms, J. Geophys. Res., 115, doi:10.1029/2009jd013430, 2010.
Wang, H., Shi, G., Zhu, J., Chen, B., Che, H., and Zhao, T.: Case study of longwave contribution to dust radiative effects over East Asia, Chinese Sci. Bull., 58, 3673–3681, doi:10.1007/s11434-013-5752-z, 2013.

Wang, H., Tan, S.-C., Wang, Y., Jiang, C., Shi, G.-y., Zhang, M.-X., and Che, H.-Z.: A multisource observation study of the severe prolonged regional haze episode over eastern China in January 2013, Atmos. Environ., 89, 807–815, doi:10.1016/j.atmosenv.2014.03.004, 2014a.

Wang, H., Xu, J., Zhang, M., Yang, Y., Shen, X., Wang, Y., Chen, D., and Guo, J.: A study of the meteorological causes of a prolonged and severe haze episode in January 2013 over central-eastern China, Atmos. Environ., 98, 146–157, doi:10.1016/j.atmosenv.2014.08.053, 2014b.

Wang, H., Shi, G. Y., Zhang, X. Y., Gong, S. L., Tan, S. C., Chen, B., Che, H. Z., and Li, T.: Mesoscale modeling study of the interactions between aerosols and PBL meteorology during a haze episode in China Jing-Jin-Ji and its near surrounding region – Part 2: Aerosols' radiative feedback effects. Atmospheric Chemistry and Physics Discussions, 14(20), 28269-28298, doi: 10.5194/acpd-14-28269-2014,2014c.

Wang, H., Xue, M., Zhang, X. Y., Liu, H. L., Zhou, C. H., Tan, S. C., Che, H. Z., Chen, B., and Li, T.: Mesoscale modeling study of the interactions between aerosols and PBL meteorology during a haze episode in Jing–Jin–Ji (China) and its nearby surrounding region – Part 1: Aerosol distributions and meteorological features. Atmospheric Chemistry and Physics, *15*(6), 3257-3275, doi: 10.5194/acp-15-3257-2015, 2015.

Wang, L., Xu, J., Yang, J., Zhao, X., Wei, W., Cheng, D., Pan, X., and Su, J.: Understanding haze pollution over the southern Hebei area of China using the CMAQ model, Atmos. Environ., 56, 69–79, doi:10.1016/j.atmosenv.2012.04.013, 2012.

Wang, L. T., Wei, Z., Yang, J., Zhang, Y., Zhang, F. F., Su, J., Meng, C. C., and Zhang, Q.: The 2013 severe haze over southern Hebei, China: model evaluation, source apportionment, and policy implications, Atmos. Chem. Phys., 14, 3151–3173, doi:10.5194/acp-14-3151-2014, 2014.

Wu, D., Tie, X., Li, C., Ying, Z., Kai-Hon Lau, A., Huang, J., Deng, X., and Bi, X.: An extremely low visibility event over the Guangzhou region: a case study, Atmos. Environ., 39, 6568– 6577, doi:10.1016/j.atmosenv.2005.07.061, 2005.

Wu, D., Wu, X. J., Li, F., Tan, J., Chen, Z. Q., Cao, X., Sun, H. H., Chen, and Li, H. Y.: Temporal and spatial variation of haze during 1951–2005 in Chinese mainland, Meteorologica Sinica, 68, 680–688, 2010.

Xu, G., Chen, D., Xue, J., Sun, J., Shen, X., Shen, Y., Huang, L., Wu, X., Zhang, H., and Wang, S.: The program structure designing and optimizing tests of GRAPES physics, Chi- nese Sci. Bull., 53, 3470–3476, doi:10.1007/s11434-008-0418-y, 2008.

Xu, H. M., Tao, J., Ho, S. S. H., Ho, K. F., Cao, J. J., Li, N., Chow, J. C., Wang, G. H., Han, Y. M., Zhang, R. J., Watson, J. G., and Zhang, J. Q.: Characteristics of fine particulate non-polar organic compounds in Guangzhou during the 16th Asian Games: effectiveness of air pollution controls, Atmos. Environ., 76, 94–101, doi: 10.1016/j.atmosenv.2012.12.037, 2013.

Xue, J., Zhuang, S., Zhu, G., Zhang, H., Liu, Z., Liu, Y., and Zhuang, Z.: Scientific design and preliminary results of three-dimensional variational data assimilation system of GRAPES, Chinese Sci. Bull., 53, 3446–3457, doi:10.1007/s11434-008-0416-0, 2008.

Yang, X., Hu, J., Chen, D., Zhang, H., Shen, X., Chen, J., and Ji, L.: Verification of GRAPES unified global and regional numerical weather prediction model dynamic core, Chinese Sci. Bull., 53, 3458–3464, doi: 10.1007/s11434-008-0417-z, 2008.

Ying, Q., Wu, L., and Zhang, H.: Local and inter-regional contributions to PM2.5 nitrate and sulfate in China, Atmos. Environ., doi:10.1016/j.atmosenv.2014.05.078, 2014.

Yu, X., Zhu, B., Yin, Y., Yang, J., Li, Y., and Bu, X.: A comparative analysis of aerosol properties in dust and haze-fog days in a Chinese urban region, Atmos. Res., 99, 241–247, doi:10.1016/j.atmosres.2010.10.015, 2011.

Zhang, R. and Shen, X.: On the development of the GRAPES – a new generation of the national operational NWP system in China, Chinese Sci. Bull., 53, 3429–3432, doi: 10.1007/s11434- 008-0462-7, 2008.

Zhang, S., Wu, Y., Wu, X., Li, M., Ge, Y., Liang, B., Xu, Y., Zhou, Y., Liu, H., Fu, L., and Hao, J.: Historic and future trends of vehicle emissions in Beijing, 1998–2020: A policy assessment for the most stringent vehicle emission control program in China, Atmos. Environ., 89, 216–229, doi:10.1016/j.atmosenv.2013.12.002, 2014.

Zhang, X. Y.: Sources of Asian dust and role of climate change versus desertification in Asian dust emission, Geophys. Res. Lett., 30, doi:10.1029/2003gl018206, 2003.

Zhou, C. H., Gong, S. L., Zhang, X. Y., Wang, Y. Q., Niu, T., Liu, H. L., Zhao, T. L., Yang, Y. Q., and Hou, Q.: Development and evaluation of an operational SDS forecasting system for East Asia: CUACE/Dust, Atmos. Chem. Phys., 8, 787–798, doi:10.5194/acp-8-787-2008, 2008.

Zhu, G., Xue, J., Zhang, H., Liu, Z., Zhuang, S., Huang, L., and Dong, P.: Direct assimilation of satellite radiance data in GRAPES variational assimilation system, Chinese Sci. Bull., 53, 3465–3469, doi:10.1007/s11434-008-0419-x, 2008.

删除的内容: ... [1]

Figure captions

Fig. 1 Mean observed and simulated PM2.5 (μg/m3) for 6–7 December 2013

Fig. 2 Simulated PM2.5 (shaded) and haze weather phenomena observed at 1400 UTC(2200 LT) 7 December 2013

Fig. 3 Mean (a) observed and (b) simulated visibility for 6–7 December 2013

Fig. 4 Daily variations in observed and simulated PM2.5 (μg/m3) for 1–31 December 2013 at stations in BJ, BD, CZ, DZ, HD, HS, NJ, SH, SJZ, XT, ZZ and the whole Jing-jin-ji

Fig. 5 (a) Horizontal wind field at 900 hPa, its vertical section at (b) 115.25°E and (c) 39.375°N at 0800 UTC(1600 LT) 7 December 2013

Fig. 6 Hourly variations in PM2.5 (μg/m3) in BJ and mean southerly wind speed (negative for northerly wind) for the region to the south of BJ, 1–10 December 2013

Fig. 7 Schematic diagram of pollutant transport between BJ and its surrounding regions

Fig. 8 PM2.5 transport rates (kg/s) from S, N, W and E of BJ on (a) 6 and (c) 7 December. Total input, output and net PM2.5 transport rate (kg/s) from BJ's environs on (b) 6 and (d) 7 December

Fig. 9 Total PM2.5 (ton) suspended in the atmosphere from the surface to 3000 m over the BJ area and the net hourly PM2.5 input (ton/h) for BJ during 6–7 December 2013

Fig. 10 Contribution made by net transport and local effects to PM2.5 increases in BJ, 6–7 December 2013

删除的内容: PK

删除的内容: , SJZ, BD, CZ, DZ, HD, HS, NJ, SH, XT and ZZ

删除的内容: PK

删除的内容: PK

删除的内容: PK

删除的内容: PK

删除的内容: PK

删除的内容: PK

删除的内容: PK

删除的内容: emissions

删除的内容: PK

Table 1 Total input, total output and total net transport (all in tons) for the BJ area for each time period (UTC and LT) during 6–7 December 2013

删除的内容: PK

Time(UTC)	Time(LT)	Input	Output	Net
0000–1200 6 Dec	0800 6 Dec-2000 6 Dec	2032	−4854	−2822
1200–2400 6 Dec	2000 6 Dec-0800 7 Dec	1850	−2617	−767
0000–1200 7 Dec	0800 7 Dec-2000 7 Dec	6551	−4288	2264
1200–2400 7 Dec	2000 7 Dec-0800 8 Dec	3523	−6653	−3130
0000–2400 6 Dec	0800 6 Dec-0800 7 Dec	3882	−7471	−3588
0000–2400 7 Dec	0800 7 Dec-0800 8 Dec	10074	−10940	−866
0000 6 Dec–2400 7 Dec	0800 6 Dec-0800 8 Dec	13956	−18411	−4455
1200 6 Dec–1200 7 Dec	2000 6 Dec-2000 7 Dec	8401	−6905	1497

Table 2 Station locations

Station	Lat.	Long.	Alt. (m)
Beijing (BJ)	39.90	116.47	31.3
Shijiazhuang (SJZ)	38.05	114.43	80.5
Baoding (BD)	38.51	115.30	17.2
Cangzhou (CZ)	38.18	116.52	9.6
Dezhou (DZ)	37.26	116.17	21.2
Handan (HD)	36.36	114.28	58.2
Hengshui (HS)	37.44	115.42	24.3
Xingtai (XT)	37.04	114.30	76.8
Zhengzhou (ZZ)	34.73	113.70	110.4
Nanjing (NJ)	32.05	118.77	8.9
Shanghai (SH)	31.23	121.48	4.5

删除的内容: PK

Fig. 1 Mean observed and simulated $PM_{2.5}$ (μg/m3) for 6–7 December 2013

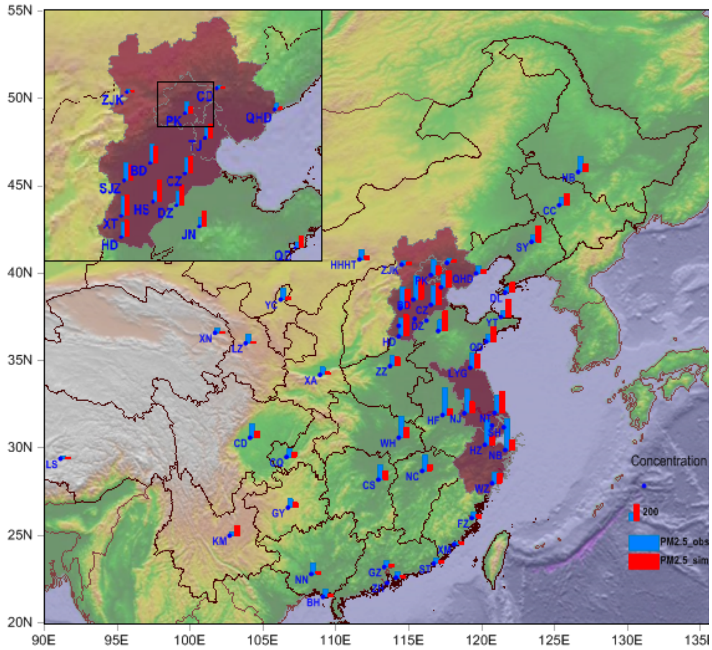

Fig. 2 Simulated $PM_{2.5}$ (shaded) and haze weather phenomena observed at 1400 UTC(2200 LT) 7 December 2013

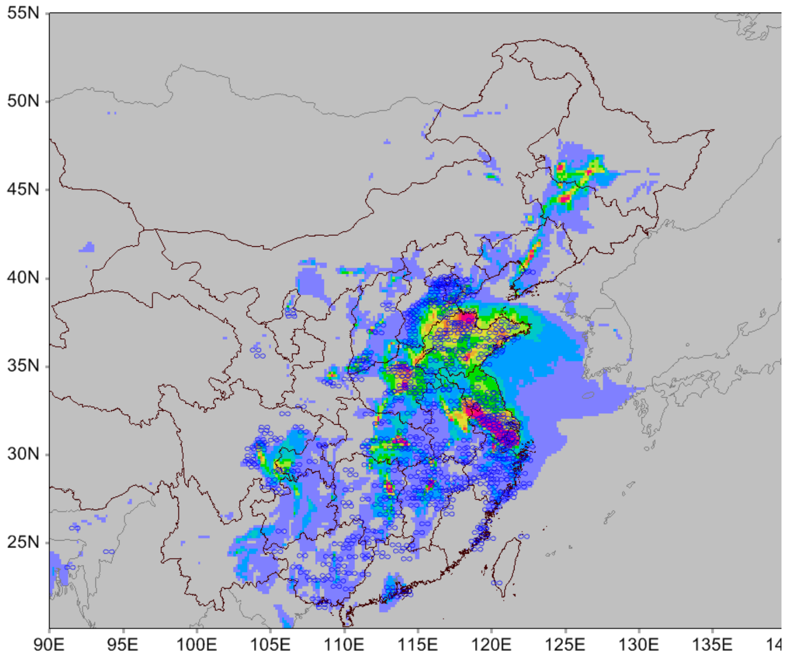

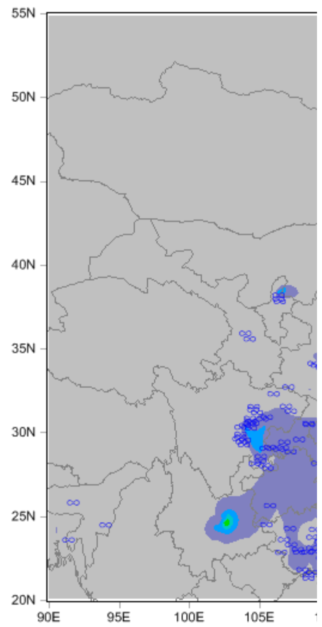

删除的内容:

带格式的: 字体:(默认) Arial

带格式的: 字体:(默认) Arial

Fig. 3 Mean observed and simulated visibility for 6–7 December 2013

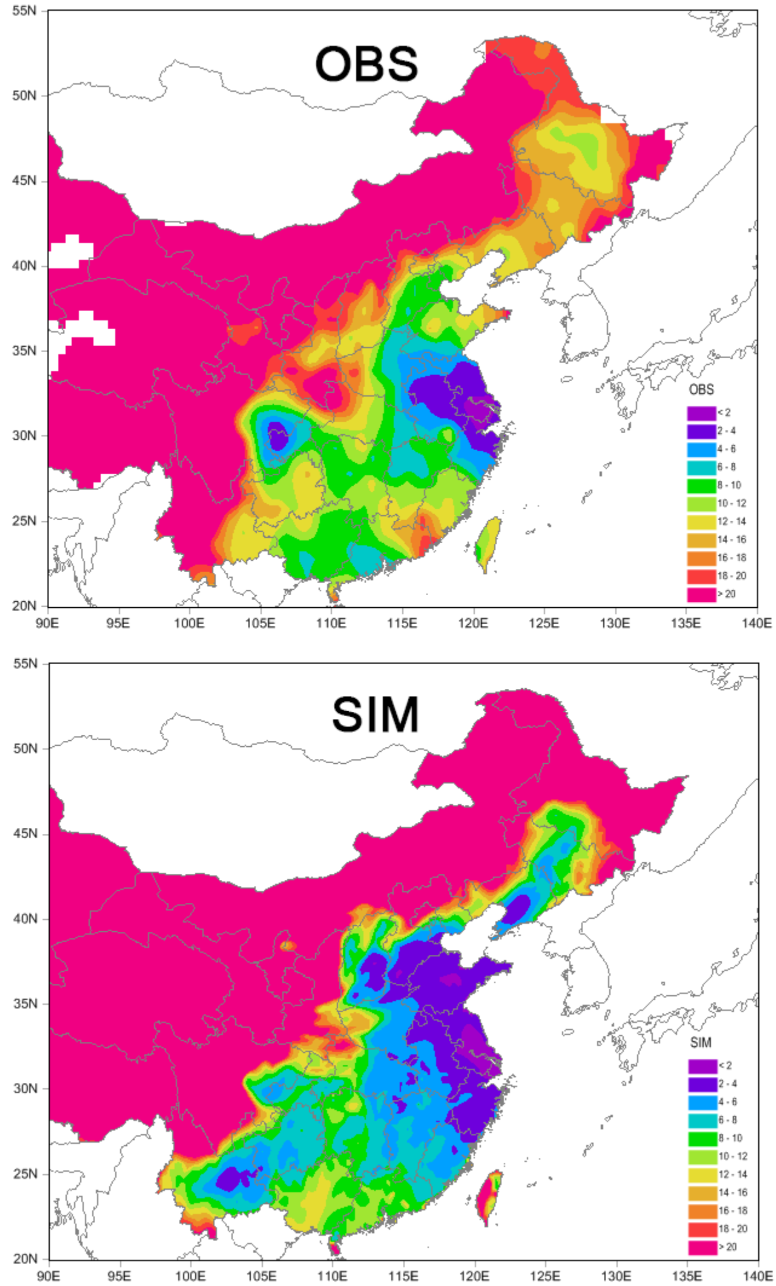

删除的内容: (a)

删除的内容: (b)

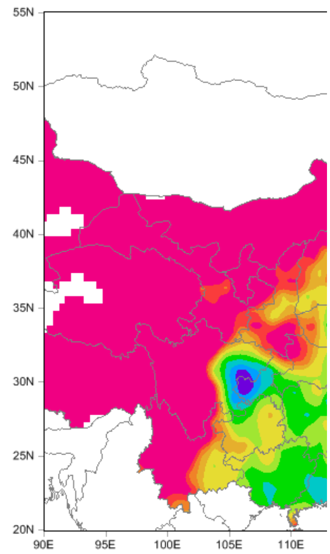

删除的内容:

带格式的: 字体:(默认) Arial

带格式的: 字体:(默认) Arial

Fig. 4 Daily variations in observed and simulated $PM_{2.5}$ (μg/m3) for 1–31 December 2013 at stations in BJ, BD, CZ, DZ, HD, HS, NJ, SH, SJZ, XT, ZZ and the whole Jing-jin-ji.

删除的内容: PK, SJZ, BD, CZ, DZ, HD, HS, NJ, SH, XT and ZZ

删除的内容:

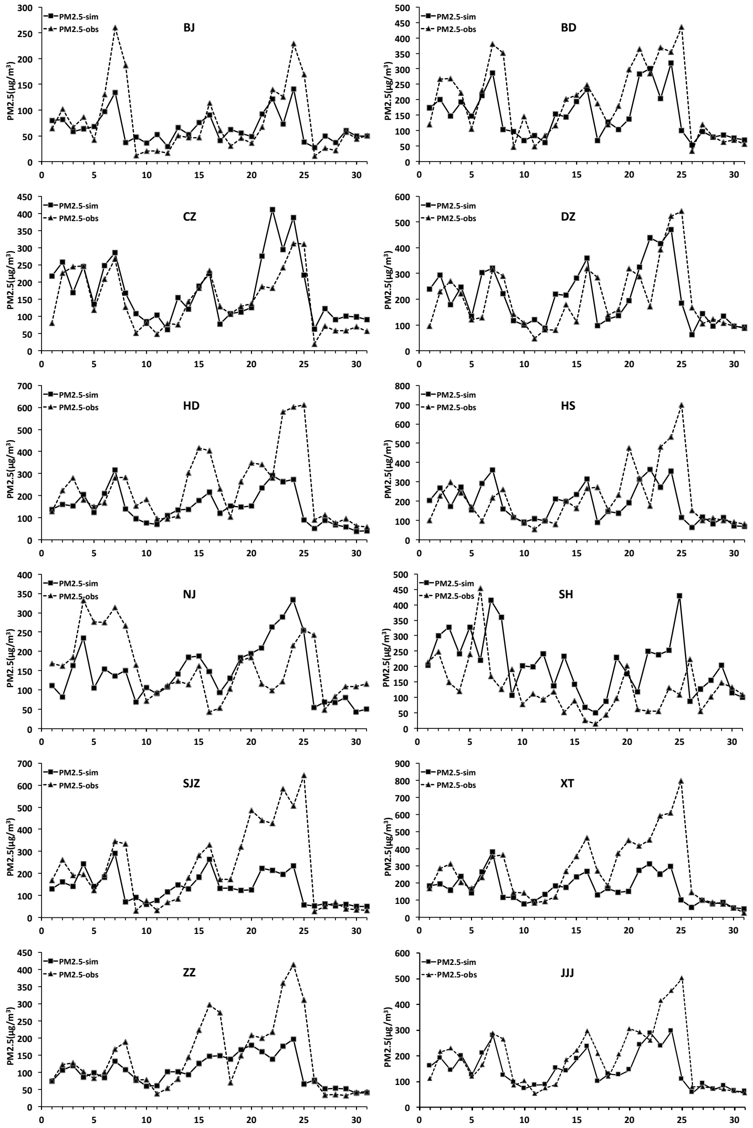

删除的内容:

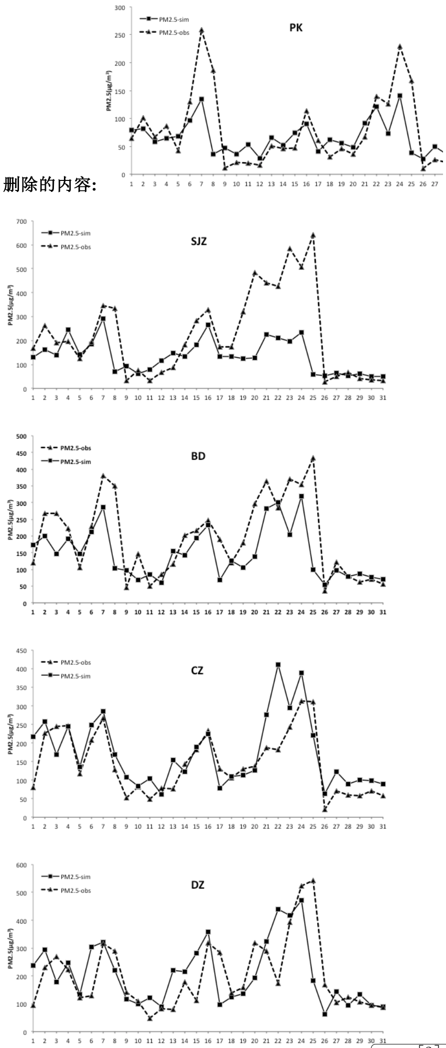

带格式的: 字体:(默认) Arial

Fig. 5 (a) Horizontal wind field at 900 hPa, its vertical section at (b) 115.25°E and (c) 39.375°N at 0800 UTC(1600 LT) 7 December 2013

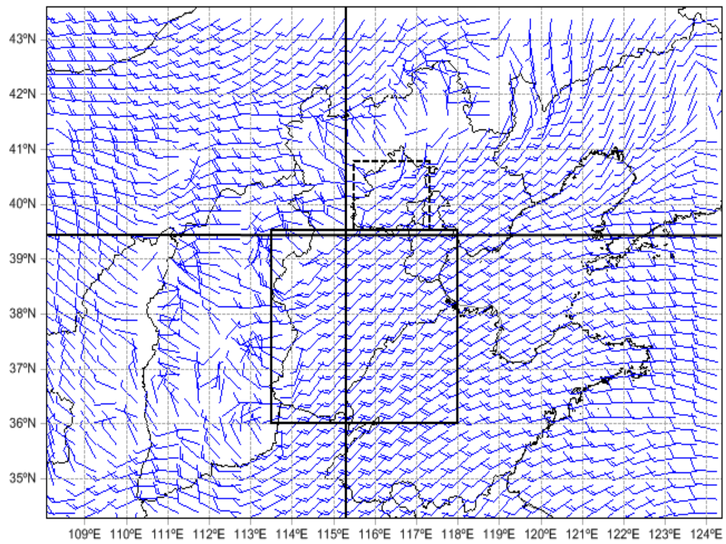

(a)

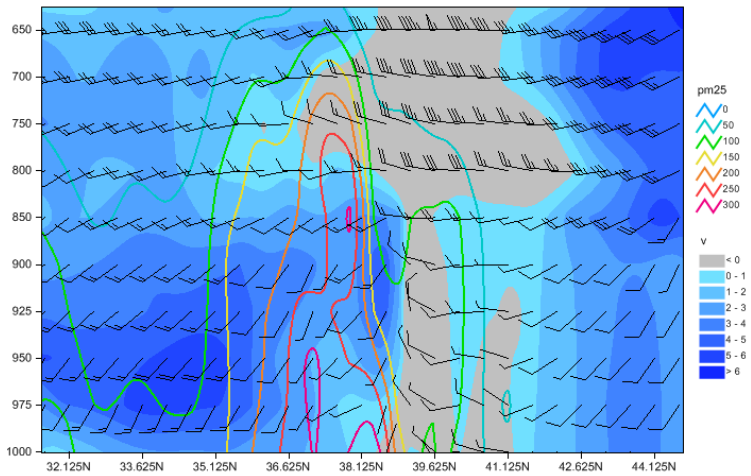

(b)

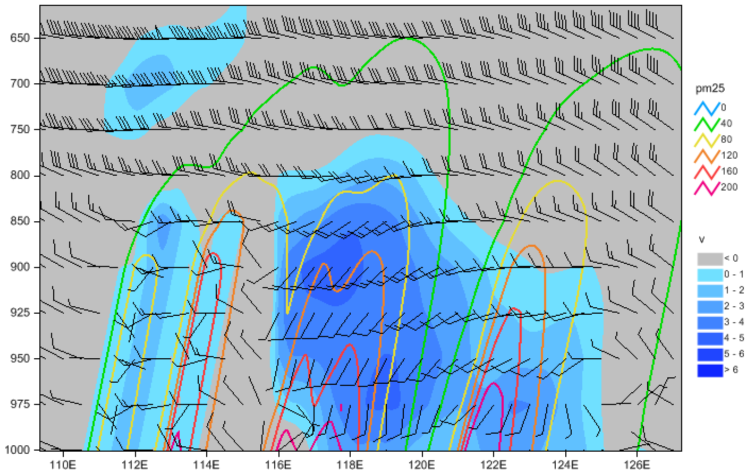
650
700
750
800
850
900
925
950
975
1000
110E
112E
114E
116E
118E
120E
122E
124E
126E
pm25
0
40
80
120
160
200
v
< 0
0 - 1
1 - 2
2 - 3
3 - 4
4 - 5
5 - 6
> 6

(c)

Fig. 6 Hourly variations in $PM_{2.5}$ (μg/m3) in BJ and mean southerly wind speed (negative for northerly wind) for the region to the south of BJ, 1–10 December 2013

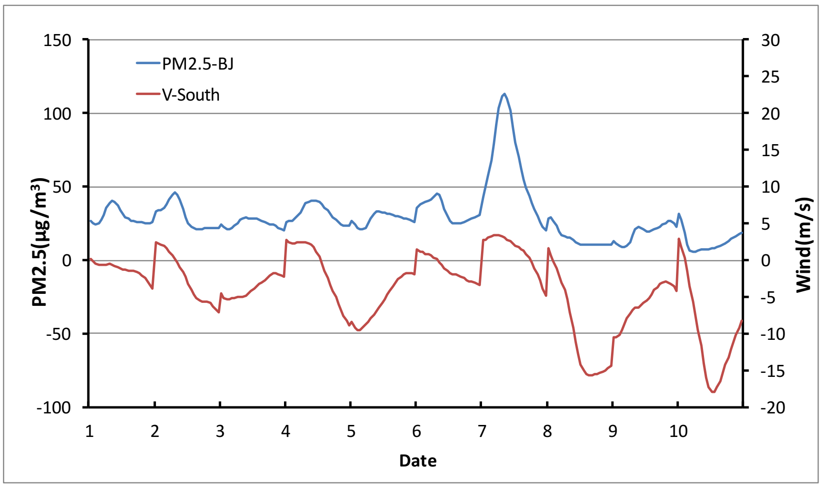

删除的内容: PK

删除的内容: PK

删除的内容:

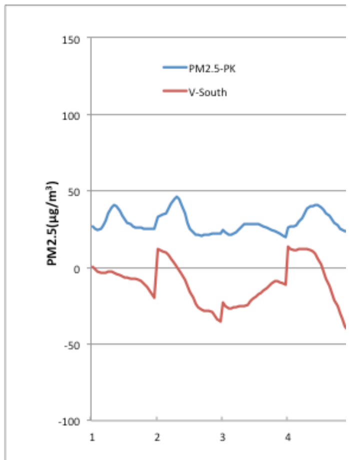

带格式的: 字体:(默认) Arial

Fig. 7 Schematic diagram of pollutant transport between BJ and its surrounding regions

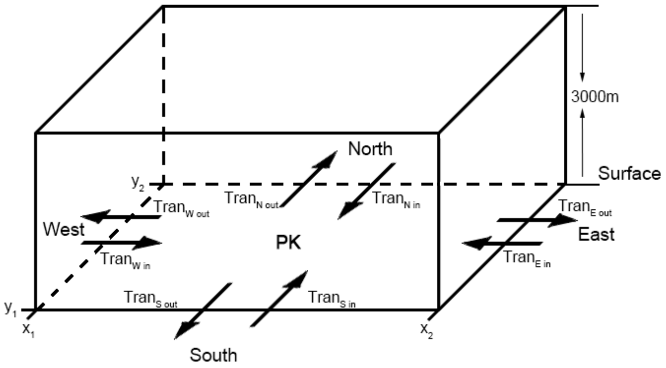

删除的内容: PK

带格式的：左对齐，孤行控制

Fig. 8 $PM_{2.5}$ transport rates (kg/s) from S, N, W and E of BJ on (a) 6 and (c) 7 December. Total input, output and net $PM_{2.5}$ transport rate (kg/s) from BJ's environs on (b) 6 and (d) 7 December

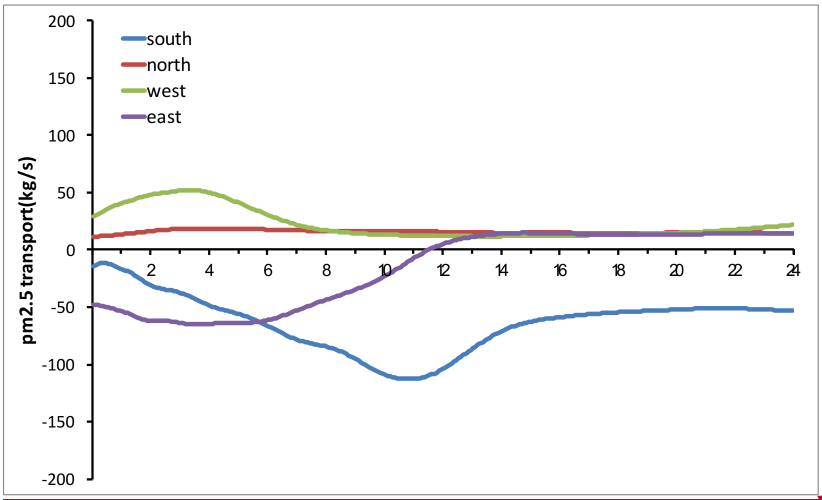

(a)

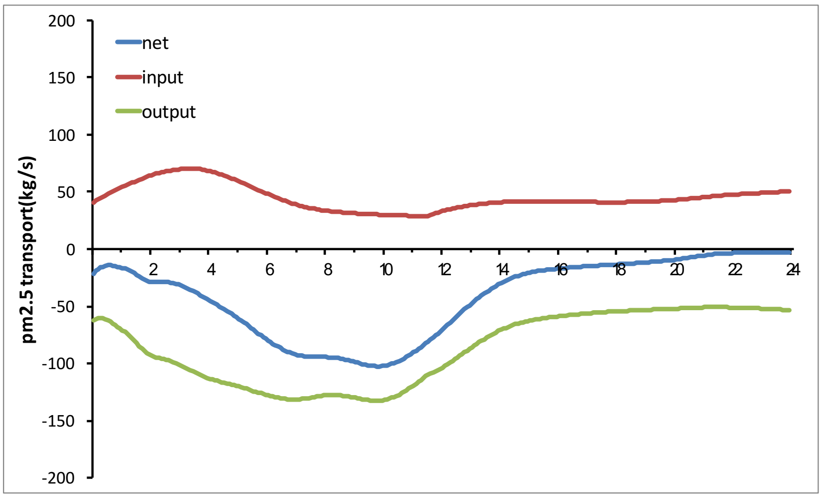

(b)

删除的内容: PK

删除的内容: PK

删除的内容:

删除的内容:

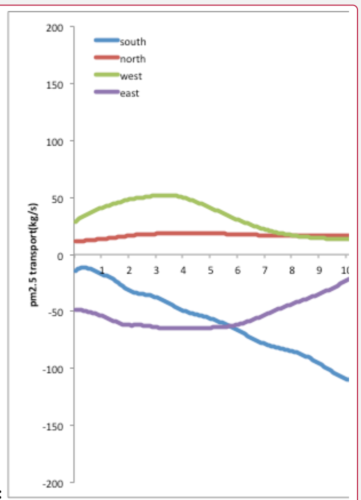

带格式的: 字体:(默认) Arial

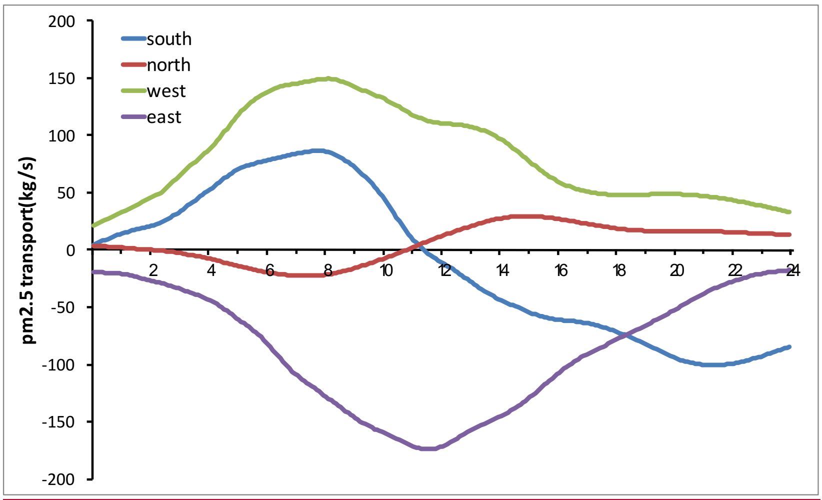

(c)

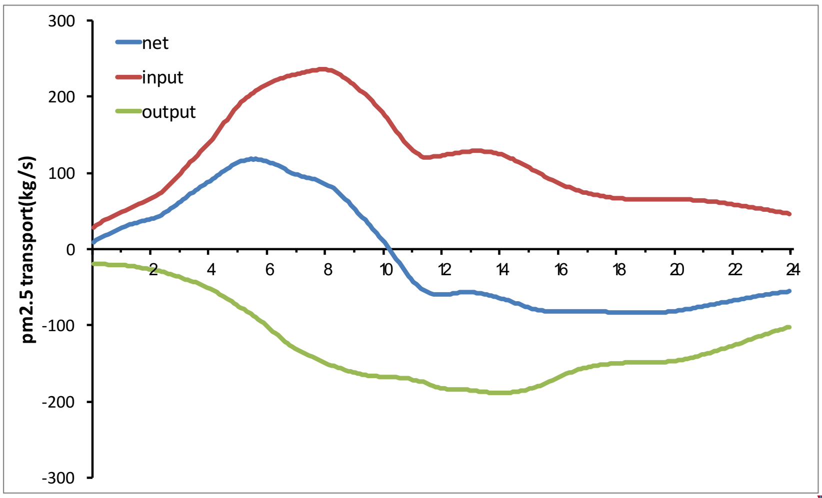

(d)

删除的内容:

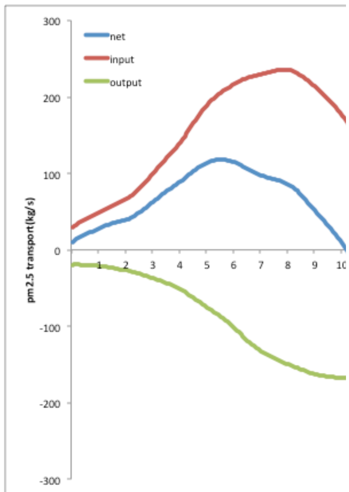

带格式的: 字体:(默认) Arial

Fig. 9 Total $PM_{2.5}$ (ton) suspended in the atmosphere from the surface to 3000 m over the BJ area and the net hourly $PM_{2.5}$ input (ton/h) for BJ during 6–7 December 2013

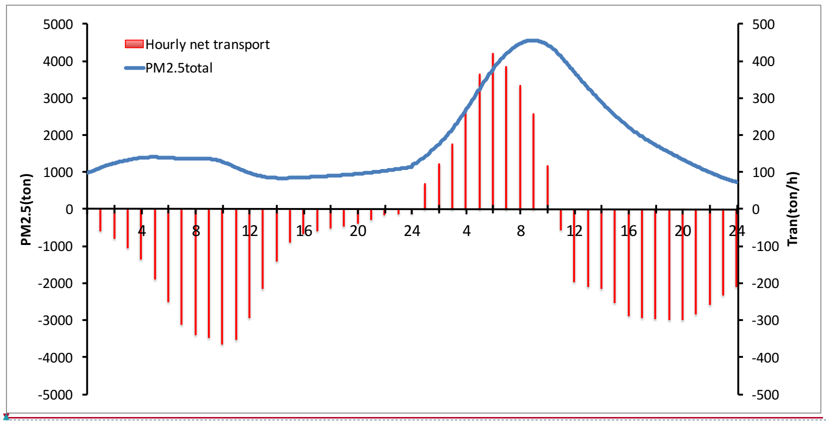

删除的内容: PK

删除的内容: PK

删除的内容:

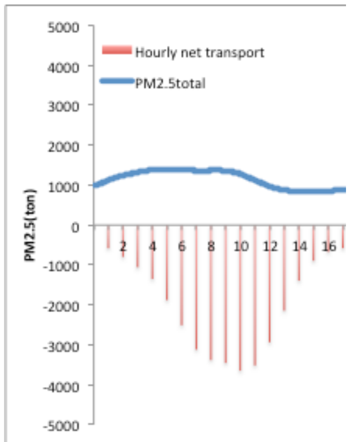

带格式的: 字体:(默认) Arial

Fig. 10 Contribution made by net transport and local effects to $PM_{2.5}$ increases in BJ, 6–7 December 2013

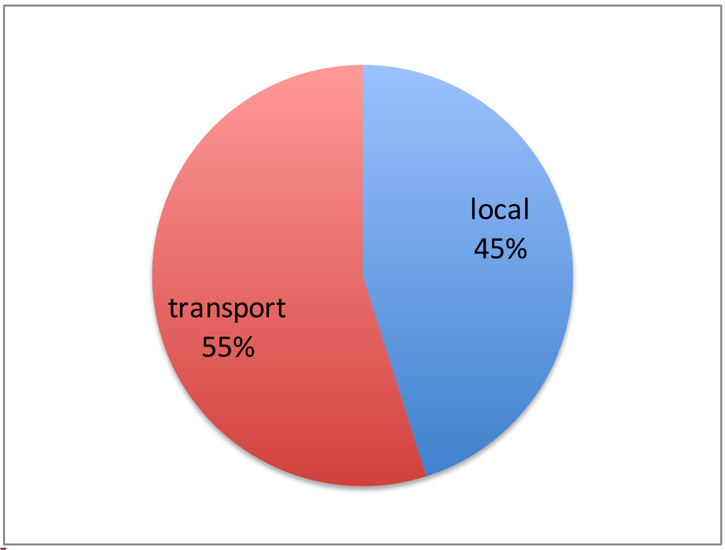

删除的内容: emissions

删除的内容: PK

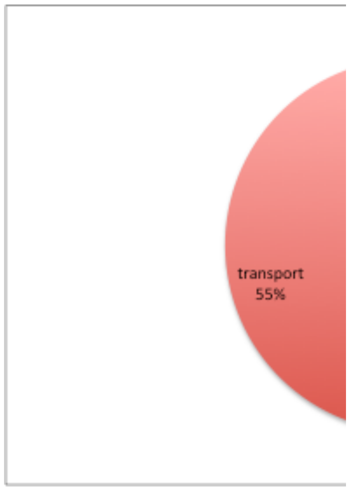

删除的内容:

带格式的: 字体:(默认) Arial